JOURNAL OF MATERIALS SCIENCE 35 (2000) 2785–2789

Concrete failure due to air-water jet impingement

A. W. MOMBER
WOMA Apparatebau GmbH, Germany
E-mail: info@woma.de

The paper reports about the generation and testing of an air-entrained waterjet for concrete demolition applications. Experimental results on concrete samples impinged by conventional waterjets and the air-waterjet show three essential features of the material removal process. First, the depth of cut is not influenced by the air addition. Second, the entrainment of air significantly affects the material removal rate. Third, there exists an optimum air flow-rate for a maximum material removal rate. Based on results of mercury-penetration measurements and acoustic-emission tests, a first phenomenological model (based on the formation of water slugs due to the air suction) is developed.

1. Introduction

High-speed waterjetting is commonly used for concrete demolition. Especially the heavy concrete removal, so-called hydrodemolition, is a suitable field for waterjet applications. An extensive application review is given in [1]. Nevertheless, as the energy efficiency of the hydrodemolition process is about 5%, investigations are required to improve the material removal performance without increasing the input energy of the waterjet generation system.

A model for the concrete destruction by high-speed waterjets is developed by the author in a series of publications [2–5]. In these papers, the influence of interfaces, cracks, and inclusions on the failure of concrete materials due to penetrating water flow at velocities of several hundred meters per second are investigated. As suggested, the predominant mechanisms of the concrete failure are the propagation and intersection of existing microcracks. It is found that the destruction process due to the high-speed water flow is introduced in the interfaces between the matrix and the aggregate grains which are characterized by a high degree of porosity and pre-existing microcracks. Inside a crack, the water is pressurized which leads to forces acting on the crack wall surface. If the generated stresses exceed critical material values, for example the critical stress intensity factor, the crack starts to grow. The crack growth is controlled by the interaction between cracks and aggregate grains. It is shown that inclusions in the material act as crack arresters and energy dissipaters [6]. The intersection of several single cracks leads to a macroscopic material removal and, finally, to the generation of fine-grained erosion debris, as discussed in [7]. In advanced versions of this phenomenological model, a computer-based simulation of the fluid dynamics inside a microcrack [8], and a fracture mechanics model of the erosion process [9] are presented. The main conclusion from these investigations is that the concrete hydrodemolition is a fracture mechanics process which involves the generation, propagation and intersection of cracks.

Air-covered waterjets have first been generated by Eddingfield and Albrecht [10] who designed and manufactured an air shroud. The idea behind their experiments was to reduce the friction between the waterjet surface and surrounding air by creating a moving air coat. During the investigations, diameter and length of the shroud are modified. The major result of this research was the discovery that the coherence of a waterjet can be improved due to the air coating. Unfortunately, no cutting or material removal experiments have been carried out to prove the expected higher efficiency of the generated air-covered waterjets.

2. Materials and experimental setup

The experiments were carried out with concrete cubes with the dimensions $150 \times 150 \times 150$ mm. The concrete was made from Portland Cement Z 35 F according to the German standard DIN 1161, and limestone as aggregate material. The water-cement-ratio was 0.45. The placing and mixing process was managed according to DIN 1048, Part 1. After mixing, the compositions were cured and hardened for 28 days under water. After hardening, the mechanical properties of the mixtures were estimated at three cylindrical specimens. These properties are listed in Table I.

For the cutting and material removal experiments, a high-pressure waterjet unit was used consisting of a plunger pump (Type 1502), a hose system, a nozzle carrier, and a rotating specimen holder. The applied pump pressure was 50 MPa and the water volume-flow rate was 75 l/min. For the mercury-penetration and acoustic-emission experiments, a pump pressure of 10 MPa was applied. Nozzle diameter and stand-off distance were 1.5 mm and 10 mm, respectively. From the rotational speed of the specimen holder, the traverse rate was estimated to be 3.5 mm/s. This corresponds to a local exposure time of about 0.43 s.

The depth of cut was estimated by averaging ten measurements along each cut. The mass loss was measured

TABLE I Mechanical parameters of the specimens

Parameter	Unit	Value
Compressive strength	MPa	39
Young's modulus	GPa	25.4
Absorbed fracture energy	MJ/m^3	65.1
Density	kg/m^3	2,290

by filling the generated cavities with fine-grained garnet sand. This sand was then removed and weighed. Since concrete is an inhomogeneous material, depth of cut and mass loss were calibrated by independent measurements at three different kerfs. In the result, a "material tolerance" value was estimated. Within this tolerance band, changes in depth of cut or mass loss are the result of the local structure of the specimens and not of external influences.

Also, the pore and crack systems of the concrete, including non-visible structural changes inside the specimens, were detected by a mercury-penetration measurement unit. Using the so-called Washburn-equation, and assuming a contact angle for concrete of $\Phi = 141.3^\circ$ [11] and the surface tension of mercury of $\sigma = 0.48$ N/m, the flaw size (pore radius respectively crack width) can be related to the known mercury penetration pressure:

$$r = \frac{7.5}{p_M} \tag{1}$$

The measurements give the cumulative distribution of the flaw volume by plotting the integrated mercury volume versus the flaw size, $V = f(r)$. In order to better understand the flaw structure, the cumulative distribution is often replaced by the differential distribution of the flaw volume, $dV/d\log r = f(r)$. This method was used in the investigation. A commercial mercury penetration unit of the Type "Carlo Erba" in a pressure range between 0.1 MPa and 200 MPa was applied. The mercury-penetration specimens had the dimensions of $8 \times 8 \times 40$ mm; they were cut away by diamond tools from the concrete samples.

Further, preliminary acoustic-emission measurements were performed by using a commercial system. The acoustic emissions caused in the specimen during the jet impingement were detected by a piezoelectric sensor (resonant frequency 500 kHz). They were converted into an electric voltage that was amplified by a pre-amplifier, and sent to a mainframe for post-processing. The sensor was fixed on the rear side of the specimen with a water-resistant epoxy.

The air-waterjet was generated in a mixing head. This head consisted of the entries for the high-speed water jet and the air flow, the mixing chamber, and the orifice for the high-speed air-waterjet. The air was sucked into the mixing chamber by the vacuum created by the high-speed water flow. The shroud system is shown in Fig. 1. The amount of air was varied by opening or closing several of the 12 air entry-holes at the circumference of the shroud.

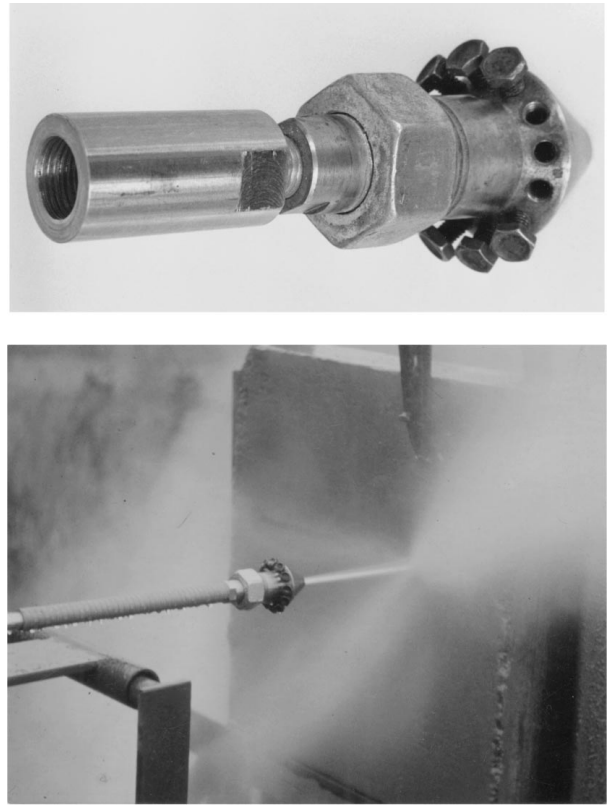

Figure 1 Air shroud system used for the investigations.

3. Experimental results

3.1. Depth of cut and material removal

The left diagram in Fig. 2 shows the influence of the air entrainment on the depth of cut. Interestingly, the depth of cut is not significantly influenced by the air addition. All estimated values are located within the material-determined tolerance band. Therefore, changes in the depth of cut are not necessarily a result of the air entrainment, but could also be a result of the material's structural inhomogeinity.

Another tendency can be observed in the right diagram of Fig. 2 showing the air influence on the material mass removal. Here, the material removal is significantly influenced by the air entrainment. The estimated values deviate from the tolerance band by sometimes 70 percent. This is the case especially if a high number of open air entry-holes is present. Assuming that a high number of open air entry-holes corresponds to a high air-flow rate, one can conclude that high air-flow rates improve the material removal capability of the investigated waterjet.

3.2. Mercury-penetration measurements

The results of the mercury-penetration measurements are shown in Fig. 3. Independent on the loading situation, all three functions peak in the flaw-size range between 20 nm and 50 nm. This region is characterized by the capillary-pore system that is generated in the hardened cement paste during the hydration. This peak is most pronounced for the unloaded concrete specimens. As the samples are subjected to waterjets, the first peak is reduced; whereas, the relative flaw volume in the microcrack-region (100 nm to 1,000 nm) increases.

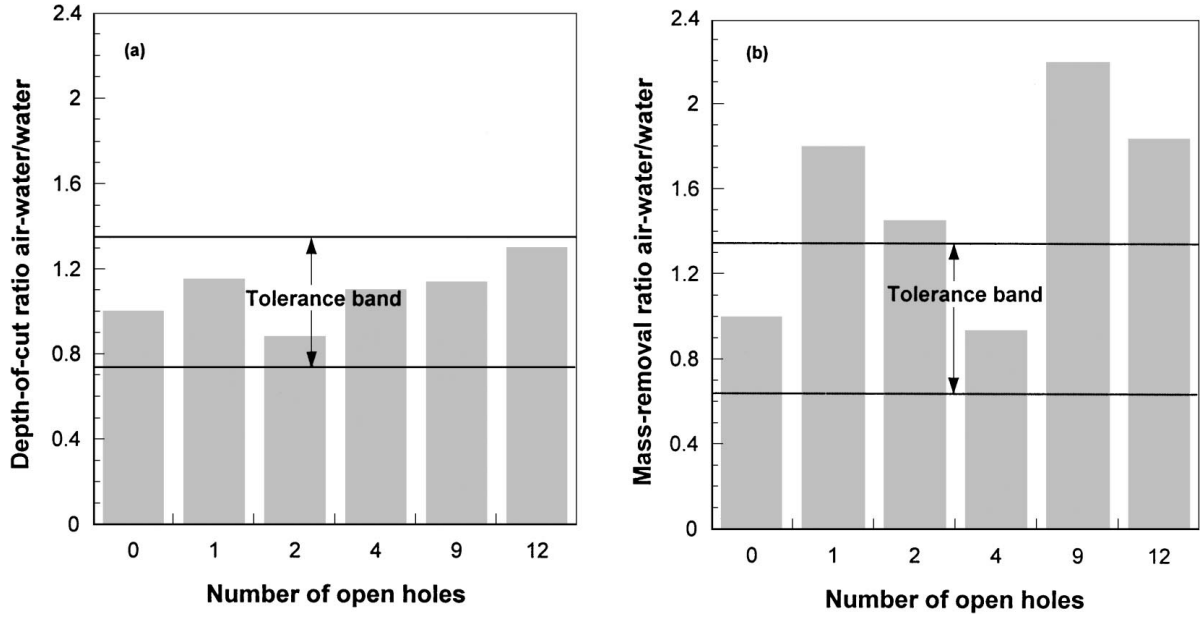

Figure 2 Relation between air entrainment and removal parameters. (a) depth of cut; (b) material mass removal.

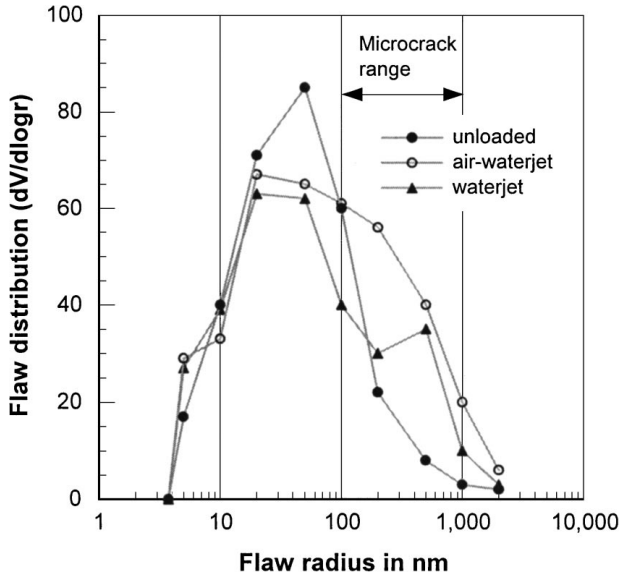

Figure 3 Results of the mercury-penetration measurements. Pump pressure: 10 MPa, nozzle diameter: 1.5 mm; number of open holes: 9.

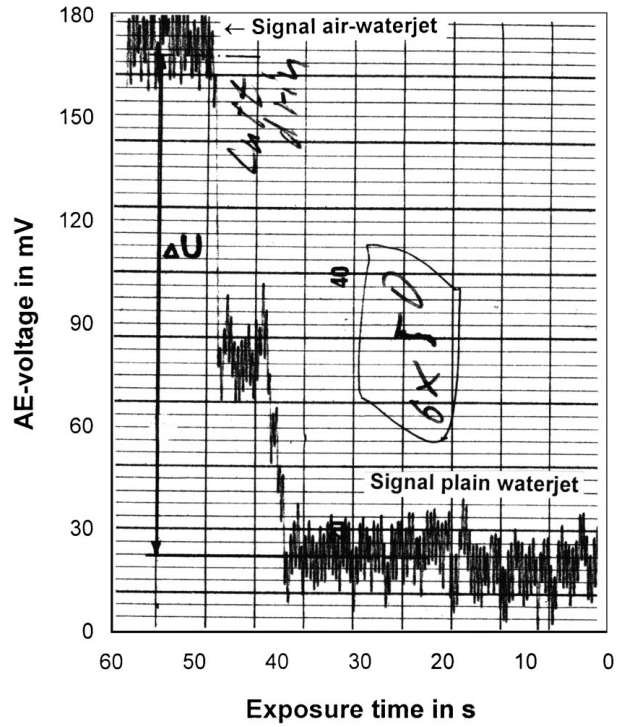

Figure 4 Acoustic-emission signals for a waterjet and an air-waterjet, respectively. Pump pressure: 10 MPa, nozzle diameter: 1.5 mm; number of open holes: 9.

Thus, a net of individual microcracks is generated in the structure due to the waterjet attack. This process is even more drastic as air-waterjets are used. Especially in the range between 1,000 nm and 2,000 nm, the amount of detected flaws is higher than for the plain waterjet. Obviously, the addition of the air leads to the generation of comparatively long cracks.

3.3. Acoustic emission measurements

Typical acoustic-emission signals are plotted in Fig. 4. On the right hand, the signal detected from a plain waterjet is shown; whereas, the left part shows the corresponding signal acquired during the impingement of the air-waterjet. Although different signal-amplifications are used, the dramatic increase in the voltage level of the signal can clearly be noticed as air is added to the waterjet. During that measurement, the voltage level increases 13-times; an average increase from five measurements is about 15-times. The voltage level of a signal from air-waterjets with a pump pressure of 10 MPa corresponds to a voltage level of a plain waterjet at a pump pressure of 35 MPa, which is a ratio of 3.5.

4. Discussion

Considering Eddington and Albrecht's [10] results, the out-come of this investigation is somewhat surprising. It does not confirm the effect of jet-bunching by the

surrounding air flow because this should lead to a better cutting capability of the jet.

It is known from several researchers that pulsating or discontinuous waterjets can substantially improve the demolition performance in concrete compared to continuous jets. Yie *et al.* [12] for example investigated concrete members under the attack of water slugs produced by high-pressure water cannons. More interestingly, Nebecker [13] found that pulsation waterjets have a higher hydrodemolition efficiency then non-affected jets. He observed that, in the case of pulsating jets, the aggregate grains in the investigated concrete specimens were broken. In contrast, they remained undamaged after conventional waterjet attack.

In the present study, the same observation has been made for the air-waterjet. This leads to the generation of a coarse-meshed crack network that allows the generation of coarse erosion debris. The reason is that neither crack-arresting nor crack-branching by the aggregates occurs. This processes have been investigated in detail in [6, 7].

Fig. 5 illustrates this phenomenon by a simple fracture mechanics model. An already existing microcrack (length 70 μm) in the cement matrix is loaded by a certain stress (level 15 MPa) generated in the crack tip by hydro-dynamic pressure. As the stress intensity is high, the crack growths and then, after 52 μm, hits an aggregate grain. At that point, the crack gets arrested if the stress does not increased. A stress level of about 100 MPa is now required to fracture the aggregate material. Thus, the pressure of the impacting waterjet needs to be increased.

This preliminary model requires the presence of a significant dynamic characteristic in the air-waterjet. It is well known that any impacting waterjet exhibits two pressure levels: an impact-pressure level in the very early moment of the jet impact (p_{IMP}), and a stagnation-pressure level (p_{ST}) that is established after the impact

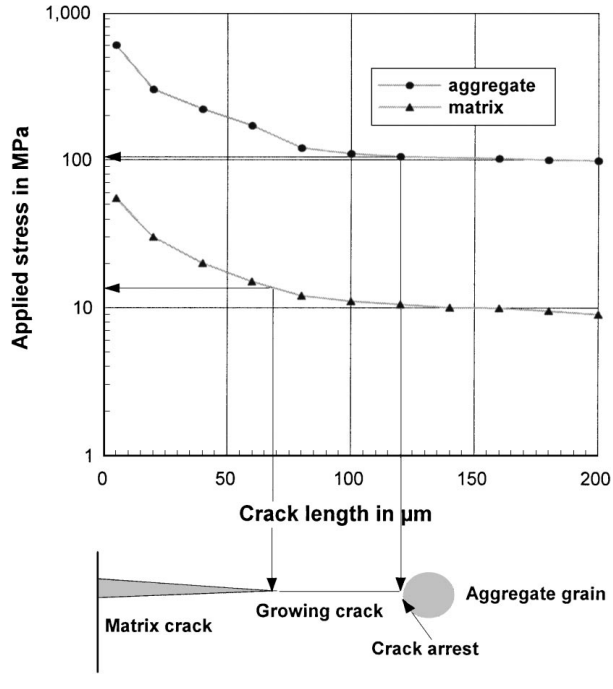

Figure 5 Fracture mechanics model; adapted from [17].

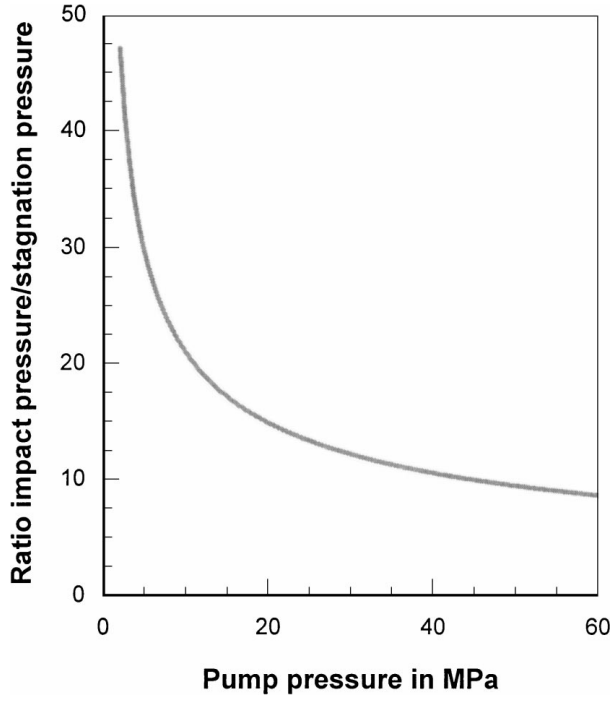

Figure 6 Relation between pressure ratio and pump pressure according to Equation 2.

period. The ratio between these pressure levels depends on the jet velocity and is given, among others, in [14]:

$$R_P = \frac{p_{IMP}}{p_{ST}} = \frac{2 \cdot 1.460}{v_{JET}} \qquad (2)$$

Results of Equation 2 are illustrated in Fig. 6 for the pressure range applied in this study. For the pump pressure of 10 MPa, the ratio between impact pressure and stagnation pressure is about $R_P = 20$. Interestingly, this ratio is in good qualitative agreement with the ratio between the voltage levels of the acoustic-emission signals of air-waterjet and waterjet ($R_{AE} = 15$), respectively. The reason for the increase in the acoustic-emission signals is the sudden energy release due to fractured aggregate grains as proven in [15] for the concrete fragmentation by abrasive-waterjets. Thus, the increase in the energy of the acoustic-emission signals if air-waterjets are used could be caused by the generation of an impact pressure suitably high to fracture the aggregate grains and to avoid crack branching or arresting, respectively. For the example in Fig. 5, the stress-amplification factor required to fracture the aggregates is $R_{ST} = 100/15 = 6.7$ which is much lower than the calculated pressure ratio R_P.

Unfortunately, no equipment was available to optically prove the assumed process of jet interruption. Nevertheless, Thorne and Theobald [16] who took high-speed photographs from waterjets, detected the disruption of a waterjet by the expansion of entrained air. As they assumed, air bubbles, already contained in the water, suddenly expanded and shattered in the jet.

5. Summary

The investigations lead to the following results:

- A simple air-shroud system for generating air-waterjets is developed and tested for concrete demolition.
- The application of the air shroud improves the material removal process significantly. In contrast, the depth of cut will not be influenced.
- The material removal process is sensitive to the amount of air sucked in. For large air flow rates, the removal process is more efficient.
- A first phenomenological model is developed based on the assumption that air bubbles in the jet suddenly expand and disrupt the jet. This results in an increase in the generated stresses due to impact pressure effects.

Acknowledgement

The author wishes to thank WOMA Apparatebau GmbH, Duisburg, for its support in preparing the paper. The investigation was partially supported by the Alexander-von-Humboldt-Foundation, Bonn, Germany.

References

1. A. W. MOMBER (ed.), "Water Jet Applications in Construction Engineering," 1st ed. (A. A. Balkema, Rotterdam, 1998).
2. A. W. MOMBER, Quecksilberporosimetriemessungen an durch Druckwasserstrahlen beanspruchten Betonproben. *Materialwiss. und Werkstofftechn.* **42** (1992) 283.
3. A. W. MOMBER and R. KOVACEVIC, *Wear* **177** (1994) 55.
4. A. W. MOMBER and H. LOUIS, *Materials and Structures*, **27** (1994) 153.
5. A. W. MOMBER and R. KOVACEVIC, AMD-Vol. 183/MD-Vol. 50 (ASME, New York, 1994) p. 327.
6. A. W. MOMBER and R. KOVACEVIC, *J. of Materials Science* **31** (1996) 1081.
7. *Idem.*, *Tribology Transact.* **39** (1996) 943.
8. A. W. MOMBER, R. KOVACEVIC and J. YE, *ibid.* **38** (1995) 686.
9. A. W. MOMBER and R. KOVACEVIC, *Int. J. of Fracture* **71** (1995) 1.
10. D. L. EDDINGFIELD and M. ALBRECHT, *ASTM STP 664*, (1979) 461.
11. K. HINRICHSMEIER, *et al.*, *Mitt. Amt. Materialprüfung Niedersachsens* **24** (1984/85) 47.
12. G. YIE, D. J. BURNS and U. H. MOHAUPT, in Proc. 4th Int. Symp. Jet Cutting Techn. edited by J. Clarke and H. S. Stephens (BHRA Fluid Engng., Cranfield, 1978) p. H6/67.
13. E. B. NEBEKER, in Proc. 7th Int. Symp. Jet Cutting Techn. edited by I. A. Walls, J. E. Stanbury (BHRA Fluid Engng., Cranfield, 1984) p. 51.
14. M. M. VIJAY, "Water Jet Applications in Construction Engineering" edited by A. W. Momber (A. A. Balkema, Rotterdam, 1998) p. 19.
15. A. W. MOMBER, R. MOHAN and R. KOVACEVIC, *Theoretical and Applied Fracture Mechanics* **31** (1999) 1.
16. P. F. THORNE and C. R. THEOBALD, in Proc. 4th Int. Symp. Jet Cutting Techn. edited by J. Clarke and H. S. Stephens (BHRA Fluid Engng., Cranfield, 1978) p. A4/55.
17. F. H. WITTMANN, *Developments in Civil Engineering* **7** (1983) 43.

Received 2 March
and accepted 11 November 1999